Photodissociation dynamics of ethylsilane: *Ab initio* and RRKM study

J. S. Francisco and H. B. Schlegel
Department of Chemistry, Wayne State University, Detroit, Michigan 48202

(Received 6 October 1987; accepted 17 November 1987)

The photodissociation dynamics of ethylsilane have been investigated by *ab initio* molecular orbital methods. Reactants, transition state structures, and products were fully optimized at HF/3-21G and HF/6-31G* levels of theory; relative energies have been calculated at MP4SDQ/6-31G*; and zero point energies and vibrational frequencies at HF/3-21G. The calculated geometries, barrier heights, and vibrational frequencies for primary dissociation channels of ethylsilane were used to compute a unimolecular dissociation rate constant $k(E)$ by RRKM theory. The barrier height of H_2 elimination (three center) is predicted to be 66.6 kcal/mol and is in good agreement with recent experimental estimates. These findings are discussed in the light of previous and recent experimental results on ehtylsilane.

I. INTRODUCTION

The infrared multiple-photon dissociation (IRMPD) of organosilanes has been observed to yield olefins, silane, and deposits of amorphous silicon (*a*:Si–H).[1] The low silane to olefin final product ratios found in these experiments, and the accompanying deposition of amorphous silicon, were attributed to secondary IRMPD of vibrationally hot silane produced in the initial photolysis step, e.g.,

$$CH_3CH_2SiH_3 \rightarrow CH_2{=}CH_2 + SiH_4 \quad (1)$$

to yield silylene (SiH_2) by

$$SiH_4 \rightarrow SiH_2 + H_2. \quad (2)$$

The primary step of this proposed mechanism involves a four-center elimination reaction of ethylsilane. Results from previous chemical activation studies of ethylsilane and ethylsilane-d_3 were congruent with these results[2,4]; however, an alternative mechanism[5] has been proposed to describe these observations, namely, a three-center elimination of molecular hydrogen in the primary step,

$$CH_3CH_2SiH_3 \rightarrow CH_3CH_2SiH + H_2 \quad (3)$$

followed by secondary IRMPD of ethylsilylene through a four-center process to yield SiH_2 and ethylene:

$$CH_3CH_2SiH \rightarrow C_2H_4 + SiH_2. \quad (4)$$

Rayner *et al.*[5] favored reactions (3) and (4), primarily because this mechanism is consistent with the major channel observed in shock-tube studies of ethylsilane.[6,7] In both mechanisms, SiH_2 is produced and may be observed by laser-induced fluorescence detection via the $\tilde{a}\ ^1B_1 \leftrightarrow \tilde{X}\ ^1A_1$ transition at 540–640 nm during the photolysis laser pulse,[5,8] which confirms the fact that SiH_2 is formed as a primary photolysis product in IRMPD experiments. However, these experiments do not provide information on the most likely channel responsible for SiH_2 formation. In order to assess the relative importance of four- and three-center elimination mechanisms represented by reactions (1) and (3), we have carried out extensive *ab initio* calculations on the ethylsilane potential surface to locate the activation barriers for each of these channels and determine their relative thermodynamic energies. We have also considered other primary processes and their importance relative to reaction (1) and (3):

$$CH_3CH_2SiH_3 \rightarrow C_2H_6 + SiH_2, \quad (5)$$

$$CH_3CH_2SiH_3 \rightarrow SiH_2{=}CHCH_3 + H_2, \quad (6)$$

$$CH_3CH_2SiH_3 \rightarrow C_2H_5 + SiH_3, \quad (7)$$

$$CH_3CH_2SiH_3 \rightarrow CH_3 + CH_2SiH_3, \quad (8)$$

$$CH_3CH_2SiH_3 \rightarrow CH_3CH_2SiH_2 + H. \quad (9)$$

With this information we comment on the photodissociation dynamics of ethylsilane in some detail.

II. COMPUTATIONAL APPROACH

Ab initio molecular orbital calculations were performed with the GAUSSIAN 82 system[9] using split valence (3-21G)[10] and polarization (6-31G*)[11] basis sets. All equilibrium geometries and transition state structures were fully optimized at the Hartree–Fock level using analytical gradient methods.[12] Electron correlation energy was estimated by the Møller–Plesset perturbation theory[13] up to fourth order, including all single, double, and quadruple excitations (MP4SDQ, frozen core). Vibrational frequencies and zero point energies were obtained from analytical second derivatives[14] calculated at the HF/3-21G level using the HF/3-21G optimized geometry.

III. COMPUTATIONAL RESULTS

A. Geometries

1. Reactant and products

The optimized geometries for all reactants and products are listed in Table I and are shown in Figs. 1 and 2. Although the geometries for some of the reactants and products have been published previously, they are reproduced here to facilitate comparison with other structures. Comparison with the available experimental structures indicates that the overall agreement is very good: $\pm$ 0.01 Å for bond lengths and $\pm$ 1° for angles at the HF/6-31G* level.

Calculated structural features for ethylsilane are compared with values derived from the microwave.[15] The calcu-

 0021-9606/88/063736-11$02.10

TABLE I. Optimized geometries of the reactants and products.[a]

	$C_2H_5SiH_3$		C_2H_5SiH		$SiH_2{=}CHCH_3$		$C_2H_5SiH_2$		CH_2SiH_3[b]	
	3-21G	6-31G*	3-21G	6-31G*	3-21G	6-31G*	3-21G	6-31G*	3-21G	6-31G*
$R(SiC_1)$	1.919	1.893	1.950	1.917	1.725	1.700	1.927	1.899	1.887	1.860
$R(C_1C_2)$	1.549	1.536	1.553	1.536	1.513	1.508	1.552	1.538		
$R(SiH_1)$	1.491	1.479	1.538	1.514	1.476	1.467			1.492	1.480
$R(SiH_2)$	1.491	1.479			1.478	1.468	1.493	1.481	1.489	1.477
$R(C_1H_4)$	1.086	1.088	1.093	1.096	1.077	1.080	1.085	1.087	1.077	1.078
$R(C_1H_5)$	1.086	1.088	1.085	1.086			1.085	1.087	1.077	1.078
$R(C_2H_6)$	1.084	1.086	1.085	1.086	1.083	1.085	1.085	1.086		
$R(C_2H_7)$	1.085	1.086	1.084	1.085	1.087	1.088	1.084	1.085		
$R(C_2H_8)$	1.085	1.086	1.086	1.087	1.087	1.088	1.084	1.085		
$\angle SiC_1C_2$	113.0	114.0	114.6	117.6	127.1	128.2	113.3	114.1		
$\angle C_1SiH_1$	111.1	110.8	95.4	96.1	122.0	121.9			111.6	111.6
$\angle C_1SiH_2$	110.3	110.5			122.1	123.0	111.7	111.5	110.2	110.1
$\angle H_1SiH_2$	108.4	108.4			115.9	115.1			108.0	108.0
$\angle H_2SiH_3$	108.2	108.2					109.5	109.0	108.9	109.1
$\angle SiC_1H_4$	108.8	108.5	106.9	104.4	117.9	116.9	108.6	108.5	122.1	122.7
$\angle SiC_1H_5$	108.8	108.5	109.6	109.5			108.6	108.5	122.1	122.7
$\angle C_2C_1H_4$	109.6	109.8	108.7	109.1	115.0	114.9	109.7	109.7	115.7	114.6
$\angle C_2C_1H_5$	109.6	109.8	109.6	109.5			109.7	109.7		
$\angle H_4C_1H_5$	106.7	105.9	106.6	105.2			106.9	106.0		
$\angle C_1C_2H_6$	110.7	111.2	110.6	111.3	112.1	112.2	110.5	111.0		
$\angle C_1C_2H_7$	111.0	111.4	110.7	111.2	110.5	111.0	111.1	111.4		
$\angle C_1C_2H_8$	111.0	111.4	111.3	111.5			111.1	111.4		
$\angle H_6C_2H_7$	107.9	107.5	108.3	108.0	108.2	107.7	108.1	107.6		
$\angle H_6C_2H_8$	107.9	107.5	107.5	107.1	108.2	107.7	108.1	107.6		
$\angle H_7C_2H_8$	108.2	107.5	108.2	107.6	107.2	107.1	108.1	107.7		
$\angle CCSiH_1$	180	180	49.2	41.6	180	180				
$\angle SiCCH_6$	180	180	179.7	179.9	0	0	180	180		

[a] Bond lengths in angstroms, angles in degrees; refer to Fig. 1 for atom numbering.
[b] $\angle H_4CSiH_1 = 89.1$ at HF/3-21G and 89.0 at HF/6-31G*.

lated values are shown in Fig. 1(a). The CC and SiH bond distances at the HF/6-31G* level are in good agreement with the experimental values (i.e., CC = 1.540 ± 0.002 Å and SiH = 1.483 ± 0.003 Å). The CSi bond length from microwave measurements is 1.866 ± 0.002 Å and compares well with the HF/6-31G* value of 1.893 Å. There is also good agreement between HF/6-31G* calculated angles and experiment; differences are generally less than ± 1°. For example, our calculated CCSi angle of 114.0° compares well with the experimental value of 113.2 ± 0.2°; likewise, for the H_1SiH_2 angle the calculated value of 108.4 agrees well with the experimental value of 108.3 ± 0.3°.

Calculations of equilibrium geometries for ethylsilylene (C_2H_5SiH) in its singlet ground state is shown in Fig. 1(c) and Table I. The computed CSi single bond lengths are 1.950 Å (3-21G) and 1.97 Å (6-31G*), which agree with previous calculations on ethylsilylene.[16] The *gauche* structure for ethylsilylene is found to be 0.79 kcal/mol higher in energy than the *trans* structure at the HF/3-21G level of theory. The CSiH angle in singlet ethylsilylene is predicted to be 95.4° (3-21G) and 96.1° (6-31G*), which is slightly greater than the HSiH angle in silylene (93.7° at HF/3-21G, 93.3° at HF/6-31G*[17], and 92.1° experimental[18]) and in methylsilylene (94.8° at HF/3-21G[19]). The larger angle in ethylsilylene as compared to silylene and methylsilylene may reflect a greater steric effect due to the ethyl group.

The geometry for 2-methylsilene ($SIH_2{=}CHCH_3$) in its singlet ground state is shown in Fig. 1(d). For some time there was a significant discrepancy between theory and experiments concerning the Si=C double bond distance; theory predicted a bond distance of 1.705 ± 0.03 Å,[20] whereas electron diffraction studies gave 1.83 ± 0.04.[21] More recently, x-ray crystallography studies[22] and theoretical calculations on silaolefins at the DZP-CI level of theory[23] show that the Si=C bond distance is 1.702 ± 0.005 and 1.703 Å, respectively. The Si=C bond distance for $SiH_2 = CHCH_3$ is overestimated at the 3-21G level of theory, while the HF/6-31G* level of theory shows good agreement with previous experimental and theoretical results.

The geometries of the $C_2H_5SiH_2$ and CH_2SiH_3 radicals optimized at HF/3-21G and HF/6-31G* levels of theory are shown in Figs. 1(b) and 1(e), respectively and in Table I. At the HF/6-31G* level of theory, the C–Si bond length in $C_2H_5SiH_2$ is 1.899 Å in this staggered structure. Further, the SiH bond length is predicted to be 1.481 Å. These calculations agree well with theoretical studies performed on CH_3SiH_2, which give the CSi bond length of 1.896 Å and SiH bond length of 1.484 Å at HF/6-31G**.[24] Our predictions for the CC bond length and CCSi angle at all levels of theory are almost identical to those in ethylsilane, which suggests that there is little delocalization of the unpaired electron across orbitals of the ethyl group in the radical. The C–Si bond length (1.860 Å) in CH_2SiH_3 agrees well with previous calculations (1.863 Å at HF/6-31G**).[24]

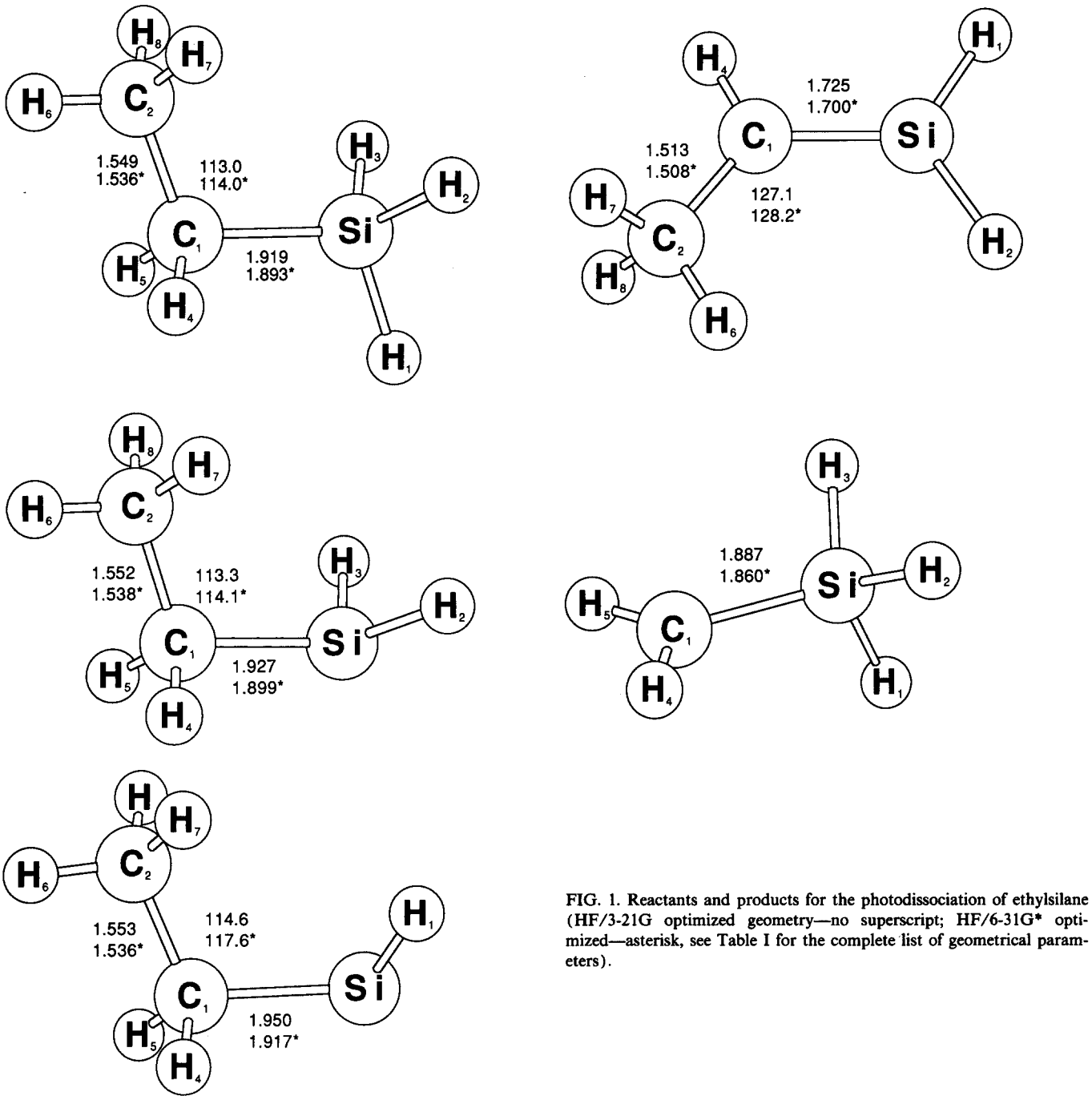

FIG. 1. Reactants and products for the photodissociation of ethylsilane (HF/3-21G optimized geometry—no superscript; HF/6-31G* optimized—asterisk, see Table I for the complete list of geometrical parameters).

2. Transition state structures

The calculated transition structure for the 1,2 elimination of SiH_4 is shown in Fig. 2(c); the full geometries are given in Table II. This pathway has a tight four-centered transition state involving the three heavy atoms and a hydrogen. The SiH_3 group must break a bond with the carbon and form a new bond with the hydrogen. These bonding changes at silicon resemble an S_N2 reaction. Similar to an S_N2 transition state, the silicon is pentacoordinated and the SiH_3 group undergoes an inversion of configuration. This process is accompanied by a lengthening of the CH bond and a shortening of the CC bond.

The optimized geometries for $C_2H_5SiH_3 \rightarrow C_2H_6 + SiH_2$ are presented in Figs. 2(a) and 2(d) and Table II. One can construct two potential transition structures of C_s symmetry (A and B). When fully optimized within C_s symmetry, structure B is lower in energy at both the HF/3-21G and HF/6-31G* levels (see total energies in Table III). However, frequency calculations reveal that neither A nor B is a true transition state, since both have two imaginary frequencies. Rotation of the CH_2CH_3 group relative to the SiH_2 reduces the symmetry to C_1 and full optimization leads to the transition structure C, which has only one imaginary frequency.

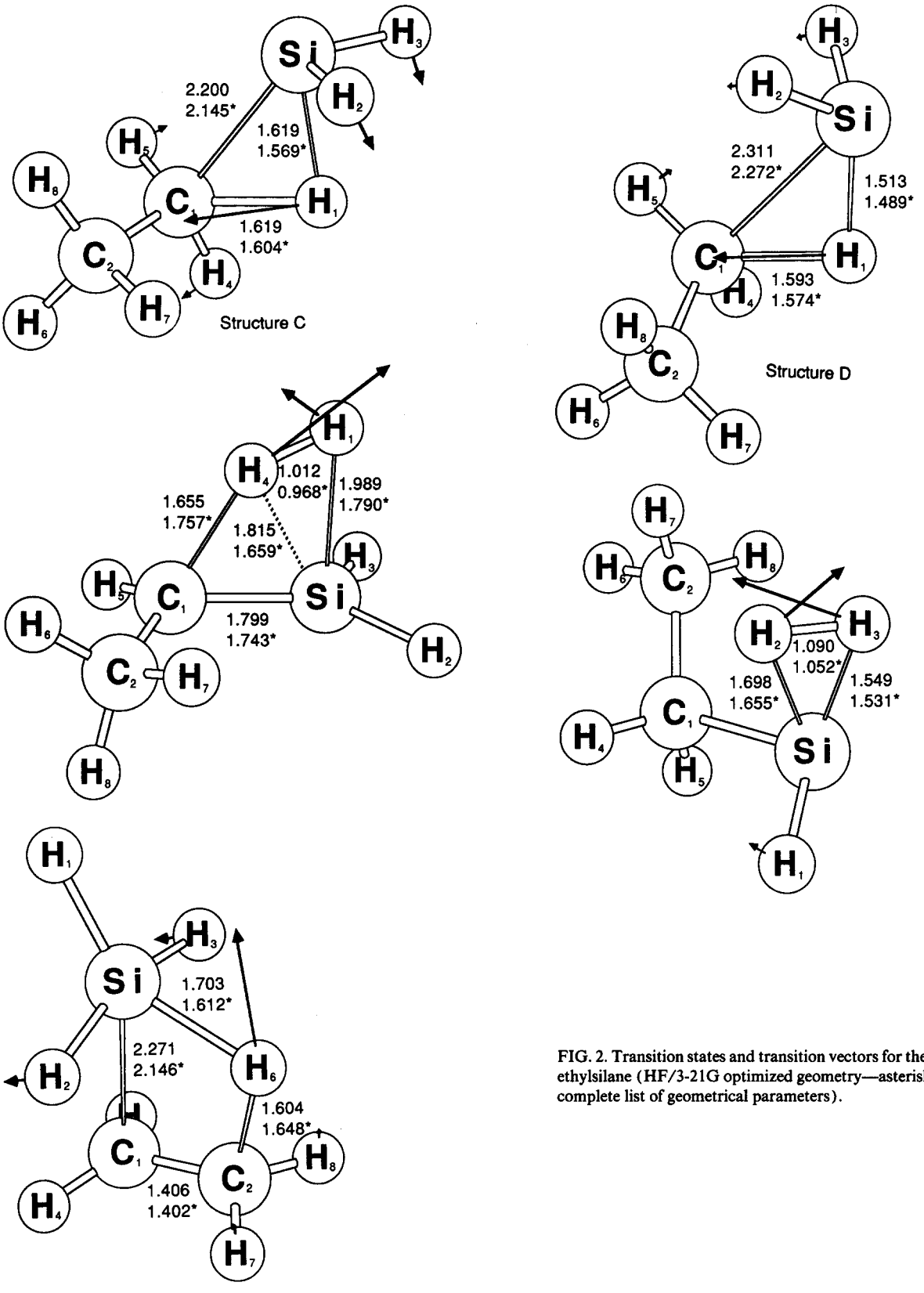

FIG. 2. Transition states and transition vectors for the photodissociation of ethylsilane (HF/3-21G optimized geometry—asterisk, see Table II for the complete list of geometrical parameters).

Comparison with the transition state for $CH_4 + SiH_2$ calculated by Gordon *et al.*[25] suggests structure D. Indeed, optimization of transition structure D yield a barrier 7.8 kcal/mol lower than structure C. The bond lengths in the transition state D for $C_2H_6 + SiH_2$ are very similar to $CH_4 + SiH_2$ [R(C–Si) = 2.305 Å, R(SiH) = 1.513 Å, R(CH) = 1.579 Å at HF/3-21G[25]]. It should be noted that both structures C and D are transition structures for $C_2H_5SiH_3 \rightarrow C_2H_6 + SiH_2$. Both possess one imaginary frequency and calculations following the reaction path[26] confirm that both

TABLE II. Optimized geometries of the transition structures.[a]

	$C_2H_5SiH_3 \rightarrow C_2H_4 + SiH_4$		$C_2H_5SiH_3 \rightarrow C_2H_6 + SiH_2$		$C_2H_5SiH_3 \rightarrow C_2H_6 + SiH_2$		$C_2H_5SiH_3 \rightarrow C_2H_5SiH + H_2$		$C_2H_5SiH_3 \rightarrow SiH_2{=}CHCH_3 + H_2$	
			Structure C		Structure D					
	3-21G	6-31G*	3-21G	6-31G*	3-21G	6-31G*	3-21G	6-31G*	3-21G	6-31G*
$R(SiC_1)$	2.271	2.146	2.200	2.145	2.311	2.272	1.942	1.921	1.799	1.743
$R(C_1C_2)$	1.406	1.402	1.530	1.521	1.532	1.521	1.548	1.535	1.526	1.517
$R(SiH_1)$	1.523	1.510	1.619	1.569	1.512	1.489	1.489	1.476	1.989	1.790
$R(SiH_2)$	1.491	1.491	1.500	1.484	1.487	1.474	1.698	1.655	1.479	1.470
$R(SiH_3)$	1.491	1.491	1.498	1.484	1.489	1.475	1.549	1.531	1.477	1.468
$R(C_1H_4)$	1.072	1.074	1.079	1.081	1.078	1.079	1.083	1.084	1.655	1.757
$R(C_1H_5)$	1.072	1.074	1.076	1.078	1.081	1.082	1.085	1.087	1.078	1.080
$R(C_2H_6)$	1.604	1.648	1.086	1.087	1.083	1.084	1.084	1.086	1.086	1.088
$R(C_2H_7)$	1.073	1.074	1.083	1.084	1.086	1.087	1.084	1.086	1.088	1.088
$R(C_2H_8)$	1.073	1.074	1.083	1.084	1.084	1.086	1.084	1.086	1.088	1.088
$\angle SiC_1C_2$	81.4	80.0	105.6	105.9	113.7	115.2	112.7	113.4	122.8	126.1
$\angle C_1SiH_1$	148.5	144.3	47.2	48.2	43.3	43.6	114.1	113.1	84.9	94.4
$\angle C_1SiH_2$	81.7	84.7	108.1	108.7	89.8	89.4	91.7	90.7	125.6	124.1
$\angle C_1SiH_3$	81.7	84.7	112.2	111.6	92.0	90.9	110.7	109.6	122.6	121.4
$\angle H_1SiH_2$	98.7	95.8	83.8	83.0	114.3	113.8	91.1	89.7	95.3	94.3
$\angle H_1SiH_3$	98.7	95.8	84.6	83.9	113.4	112.9	111.5	110.7	95.4	94.4
$\angle H_2SiH_3$	162.3	168.3	110.1	109.7	110.0	110.1	38.9	38.3	111.5	112.7
$\angle SiC_1H_4$	106.7	108.7	122.0	122.0	94.5	94.8	110.3	110.6	63.3	56.6
$\angle SiC_2H_5$	106.7	108.7	96.0	97.5	113.0	111.9	107.2	107.3	116.0	116.3
$\angle C_2C_1H_4$	118.8	118.2	111.1	110.5	112.2	112.2	110.0	110.1	113.8	113.7
$\angle C_2C_1H_5$	118.8	118.2	112.9	113.3	112.9	112.8	109.1	108.9	115.7	116.1
$\angle H_4C_1H_5$	116.2	115.8	108.4	107.3	109.1	108.5	107.3	106.2	113.9	110.2
$\angle C_1C_2H_6$	107.3	107.2	108.9	109.1	110.1	110.2	110.3	110.7	109.6	111.6
$\angle C_1C_2H_7$	119.7	120.3	111.2	111.4	111.5	111.9	111.0	111.5	111.7	111.9
$\angle C_1C_2H_8$	119.7	120.3	111.0	111.5	110.9	111.3	111.1	111.7	113.6	112.7
$\angle H_6C_2H_7$	91.8	90.3	108.0	107.6	107.9	107.6	107.9	107.4	107.0	106.6
$\angle H_6C_2H_8$	91.8	90.3	109.0	108.8	108.0	107.8	108.1	107.6	107.3	107.0
$\angle H_7C_2H_8$	116.0	116.0	108.6	108.3	108.2	107.8	108.4	107.7	107.4	106.7
$\angle CCSiH_1$	180	180	101.2	106.4	72.6	70.3	150.6	150.5	−100.9	−95.4
$\angle SiCCH_6$	0	0	175.4	178.1	168.6	169.3	176.2	176.1	151.7	137.7

[a] Bond lengths in angstroms, angles in degrees; refer to Fig. 2 for atom numbering.

connect $C_2H_5SiH_3$ and $C_2H_6 + SiH_2$.

The addition of molecular hydrogen to ethylsilylene via a three-centered transition state is the reverse of reaction (3), the 1,1 elimination of H_2 from ethylsilane. These reactions are considered prototypical for the reactions involving organosilane decompositions.[6] The optimized geometries for the transition state for $C_2H_5SiH + H_2$ are given in Fig. 2(e) and Table II. The ethylsilylene insertion shows a larger increase in the H_2 bond length and is very similar to the increase in the H_2 bonds in the silylene insertion into H_2 [R(H–H) = 1.052 Å vs 1.092 Å, respectively, at HF/6-31G*]. The Si–H distances are somewhat longer for the ethylsilylene insertion than for silylene insertion [R(Si–H) = 1.531, 1.655 Å vs 1.520, 1.638 Å, respectively, at HF/6-31G*].

The transition structure for the 1,2 elimination of H_2 is shown in Fig. 2(b). The SiH_2CHCH_3 fragment in the transition structure is quite similar to the product, indicative of a late transition state. The breaking of the CH and SiH bonds occurs unsymmetrically, leading to a rather distorted four-center transition state. A similar distortion is found for 1,2 hydrogen elimination in C_2H_6,[27] Si_2H_6[28], and CH_3SiH_3,[29] and is a consequence of the orbital symmetry forbidden nature of these reactions. These transition states can perhaps be described as a combination of a 1,2 hydrogen shift and a 1,1 elimination of H_2.

B. Vibrational frequencies

The HF/3-21G harmonic vibrational frequencies for ethylsilane and its various transition state structures are listed in Table IV. Ethylsilane in its staggered configuration possesses C_s symmetry and its vibrations span the representation,

$$\Gamma = 16a' + 11a''.$$

All vibrations in this representation are infrared and Raman active. Calculated frequencies of ethylsilane compared to experimental ones[30,31] are overestimated by ~10%–15% owing to the use of the harmonic approximation, of the truncation of the basis set, and to neglect of electron correlation in the HF/3-21G frequency calculation.[32] Nevertheless, the calculated frequencies appear in the correct order. The largest errors are primarily in the Si–H and C–H stretching frequencies, while the lower frequency (deformations, rocks, and torsion) modes show better agreement with experiment.

TABLE III. Total energies.[a]

System	HF/3-21G	HF/6-31G*	MP2/6-31G*	MP3/6-31G*	MP4/6-31G*
			$C_2H_5SiH_3$		
Reactant	− 367.341 64	− 369.303 04	− 369.646 46	− 369.664 32	− 369.692 67
			$C_2H_5SiH_3 \rightarrow C_2H_4 + SiH_4$		
Transition structure	− 367.166 55	− 369.139 62	− 369.499 51	− 369.534 39	− 369.544 04
Product	− 367.287 97	− 369.256 85	− 369.591 37	− 369.630 76	− 369.640 65
			$C_2H_5SiH_5 \rightarrow C_2H_6 + SiH_2$		
Transition structures					
A	− 367.186 42	− 369.143 29	− 369.509 60	− 369.549 09	− 369.558 67
B	− 367.189 78	− 369.145 48	− 369.510 77	− 369.550 22	− 369.559 98
C	− 367.191 69	− 369.147 24	− 369.512 92	− 369.552 47	− 369.561 98
D	− 367.207 78	− 369.160 54	− 369.527 51	− 369.565 06	− 369.574 72
Product	− 367.278 24	− 369.228 48	− 369.561 57	− 369.604 74	− 369.615 11
			$C_2H_5SiH_3 \rightarrow C_2H_5SiH + H_2$		
Transition structure	− 367.214 50	− 369.168 36	− 369.533 20	− 369.573 67	− 369.582 20
Product	− 367.263 76	− 369.203 67	− 369.552 33	− 369.593 57	− 369.603 70
			$C_2H_5SiH_3 \rightarrow SiH_2{=}CHCH_3 + H_2$		
Transition structure	− 367.130 77	− 369.104 00	− 369.467 25	− 369.501 49	− 369.510 45
Product	− 367.243 47	− 369.198 36	− 369.560 59	− 369.596 61	− 369.606 70
			$C_2H_5SiH_3 \rightarrow C_2H_5 + SiH_3$		
Product	− 367.244 18	− 369.203 27	− 369.509 82	− 369.552 08	− 369.561 44
			$C_2H_5SiH_3 \rightarrow C_2H_5SiH_2 + H$		
Product	− 367.229 65	− 369.180 87	− 369.511 21	− 369.546 62	− 369.554 54
			$C_2H_5SiH_3 \rightarrow CH_3 + CH_2SiH_3$		
Product	− 367.239 60	− 369.202 73	− 369.496 03	− 369.540 98	− 369.550 18

[a]Total energies in a.u., 1 a.u. = 627.51 kcal/mol.

TABLE IV. Vibrational frequencies.[a]

Reactant	Transition structures						
				$C_2H_5SiH_3 \rightarrow C_2H_6 + SiH_2$			
$C_2H_5SiH_3$[b]	$C_2H_5SiH_3 \rightarrow C_2H_3SiH + H_2$	$C_2H_5SiH_3 \rightarrow C_2H_4 + SiH_4$	$C_2H_5SiH_3 \rightarrow SiH_2{=}CHCH_3 + H_2$	A	B	C	D
126 a'' (150;140)[c]	1710i	1472i a'	2742i	1339i a'	1382i a'	1412i	1539i
232 a'' (215)	132	304 a'	55	209i a''	109i a''	128	102
266 a' (221)[c]	247	344 a''	72	295 a''	275 a''	246	204
562 a'' (515)	287	443 a'	253	320 a'	364 a'	266	293
627 a' (602)	562	578 a'	491	410 a''	452 a'	450	437
729 a' (691)	633	676 a''	532	488 a'	459 a''	632	656
846 a'' (764)	703	836 a''	626	799 a''	795 a''	772	663
996 a' (933)	840	913 a'	756	844 a'	816 a'	869	821
1015 a' (1026)	854	945 a''	831	867 a''	915 a''	909	935
1028 a'' (933)	1014	1024 a''	906	943 a'	948 a'	968	1011
1034 a' (942)	1103	1056 a'	992	984 a'	1000 a'	1011	1020
1113 a'' (979)	1135	1148 a'	1118	1191 a'	1139 a''	1134	1074
1140 a' (979)	1144	1261 a'	1136	1232 a''	1156 a'	1200	1170
1400 a'' (1241)	1399	1261 a''	1172	1382 a'	1343 a'	1343	1318
1410 a' (1241)	1407	1317 a''	1388	1482 a''	1412 a''	1384	1379
1577 a' (1382)	1540	1355 a'	1448	1568 a'	1579 a'	1583	1581
1623 a' (1417)	1577	1376 a''	1497	1610 a'	1597 a'	1643	1631
1674 a' (1465)	1643	1605 a'	1587	1655 a''	1665 a''	1660	1668
1681 a'' (1472)	1675	1636 a'	1670	1661 a'	1666 a'	1672	1671
2252 a'' (2158)	1680	1671 a'	1684	1885 a'	2000 a'	1913	2242
2255 a' (2164)	2096	2037 a'	1747	2190 a'	2212 a'	2199	2275
2268 a' (2171)	2267	2169 a'	2312	2207 a''	2235 a''	2224	2286
3192 a' (2890)	3197	2226 a''	2328	3173 a'	3198 a'	3200	3193
3197 a' (2935)	3211	3320 a'	3156	3257 a'	3262 a'	3256	3243
3229 a'' (2978)	3248	3338 a'	3186	3281 a'	3287 a''	3266	3259
3251 a' (2964)	3254	3407 a''	3236	3307 a''	3292 a'	3294	3268
3257 a'' (2969)	3273	3434 a''	3311	3332 a''	3367 a''	3334	3326

[a]Harmonic vibrational frequencies in cm^{-1} calculated at the HF/3-21G level.
[b]Observed anharmonic frequencies in parentheses taken from Ref. 28.
[c]Data taken from Ref. 29.

The vibrational frequencies for the transition structures are all characterized by one imaginary frequency. Those for the 1,1-H_2 elimination reaction (3) closely resemble those of ethylsilane. The imaginary frequency is quite large ($1710i$ cm^{-1}) and is consistent with a narrow barrier; the nature of the transition vector for silane decomposition[33] is similar. In the transition structure for 1,2-SiH_4 elimination, the transition vector consists mainly of a CH stretching mode mixed with the SiH_3 umbrella motion. The remaining frequencies of the transition structure, for the most part, lie between the frequencies of the reactants and products. For the $SiH_2{=}CHCH_3 + H_2$ transition state, the normal mode with a frequency of $2742i$ cm^{-1}, can be described as a CH stretch in the SiCH plane mixed with the SiH stretch in the CSiH plane. Most of the remaining modes for this structure mimic those of the product with the exception of two very low frequency modes which correspond to SiH_3 rock mixed with $C(CH_3)H_2$ torsion (55 cm^{-1}) and SiH_3 torsion mixed with $H \cdots CH(CH_3)$ twisting motion. The transition vector for the three-center elimination of SiH_2 for structure C corresponds to a 1,2 hydrogen shift mixed with SiH_3 rotation. While that for the structure D appears to be distinctly different; it corresponds more to hydrogen addition from SiH_3 into C_2H_5, but this pathway is well below the energetic level of structure D and that for the $C_2H_5 + SiH_3$ reaction.

C. Relative energies

1. Thermodynamics

The ΔH_f° for SiH_4 of 8.1 ± 0.5 kcal/mol is obtained from the decomposition of silane.[34] Doncaster and Walsh have determined the heat of formation for SiH_3 [35] as 46.6 ± 1.4 kcal/mol, and this is consistent with results from photoionization studies on SiH_4.[36] The experimental heat of formation for SiH_2 has been determined by Francisco *et al.* as 63.6 ± 2.8 kcal/mol.[37] The $\Delta H_f^\circ(C_2H_4)$ is 12.54 ± 0.07 kcal/mol,[38] and that for C_2H_6 is -20.0 ± 0.1 kcal/mol.[39] The $\Delta H_f^\circ(C_2H_5)$ normally accepted, 25.9 ± 1.3 kcal/mol,[40] is too low; and we use the higher value for $\Delta H_f^\circ(C_2H_5)$ of 28.0 ± 1.0 kcal/mol[41,42] which resolves conflicting data on the self-reaction of ethyl radical.[43] There are no experimental measurements for the heats of formation of C_2H_5SiH, $SiH_2{=}CHCH_3$, CH_2SiH_3, and $CH_3CH_2SiH_3$. Nevertheless, Rickborn *et al.*[7] have estimated $\Delta H_f^\circ(C_2H_5SiH_3)$ as -11.2 kcal/mol. Their value is derived from the simple thermodynamic relationship

$$\Delta H_f^\circ(C_2H_5SiH_3) = \Delta H_f^\circ(C_2H_5) + \Delta H_f^\circ(SiH_3) - D(\text{Si–C})$$

in which values for $\Delta H_f^\circ(C_2H_5) = 26.5$ kcal/mol, $\Delta H_f^\circ(SiH_3) = 46.4$ kcal/mol, and a carbon–silicon bond dissociation energy D(Si–C) of 84 kcal/mol are used. The carbon–silicon bond dissociation energy used by the authors is derived from measurements of the bond dissociation energy in Me_3Si–CH_3 [44] and related compounds.[45] However, D(Si–C) assumed by Rickborn and co-workers is larger than the experimentally measured carbon–silicon bond dissociation for ethylsilane of 75 ± 4 kcal/mol from chemical activation studies.[3] If we use $D(\text{Si–C}) = 75 \pm 4$, $\Delta H_f^\circ(C_2H_5) = -0.4 \pm 4.4$ kcal/mol.

The theoretical heat of reaction for ethylsilane dissociation into $C_2H_5 + SiH_3$ represented by the breaking of an Si–C bond is given in Table V and is in excellent agreement with experiment. This we believe offers support for the estimated value for $\Delta H_f^\circ(C_2H_5SiH_3) = -0.4 \pm 4.4$ kcal/mol. Comparison of the experimental heats of reactions determined with the newly estimated $\Delta H_f^\circ(C_2H_5SiH_3)$ value provides an internally consistent set of heat of reaction data. For example, the reaction yielding $C_2H_6 + SiH_2$, the experimental ΔH° of 44.0 kcal/mol compares well to our theoretical estimate of 46.2 kcal/mol as shown in Table V. On the other hand, using $\Delta H_f^\circ(C_2H_5SiH_3) = -11.2$ kcal/mol shows a 8.6 kcal/mol discrepancy. The calculated ΔH° for $C_2H_5SiH \rightarrow C_2H_4 + SiH_4$ is 27.4 kcal/mol and compares favorably with the experimental estimate of 21.1 kcal/mol. In general, the deviation between the experimental heats of reactions calculated with $\Delta H_f^\circ(C_2H_5SiH_3) = -0.4$ kcal/mol and theoretical heats of reactions from this work is ~ 3 kcal/mol.

On purely thermodynamic grounds, the energetically most favorable reaction is clearly four-center elimination of SiH_4 to form ethylene. The 1,2 hydrogen shift to yield SiH_2 and C_2H_6 is the next thermodynamically favorable reaction. While the 1,2 elimination of H_2 from ethylsilane is thermodynamically competitive with reaction (4), it is predicted to be 0.5 kcal/mol less favorable. The heat of reaction for three-center elimination of $C_2H_5SiH + H_2$ is higher than that for

TABLE V. Heats of reaction.[a]

Level of theory	$C_2H_5SiH_3 \rightarrow C_2H_4 + SiH_4$	$C_2H_5SiH_3 \rightarrow C_2H_6 + SiH_2$	$C_2H_5SiH_3 \rightarrow C_2H_5SiH + H_2$	$C_2H_5SiH_3 \rightarrow SiH_2{=}CHCH_3 + H_2$	$C_2H_5SiH_3 \rightarrow C_2H_5 + SiH_3$	$C_2H_5SiH_3 \rightarrow C_2H_5SiH_2 + H$	$C_2H_5SiH_3 \rightarrow CH_3 + CH_2SiH_3$
3-21G	33.7	39.8	48.9	61.6	61.2	70.3	64.0
6-31G*	29.0	46.8	62.4	65.7	62.6	76.7	62.9
MP2/6-31G*	34.6	53.3	59.1	53.9	85.7	84.9	94.2
MP3/6-31G*	33.6	49.9	56.9	55.0	83.0	86.4	90.0
MP4/6-31G*	32.6	48.7	55.8	53.9	82.4	86.7	89.4
ΔZPE/3-21G	5.2	2.5	5.6	7.2	6.5	6.2	9.7
ΔH_f°, 0 K							
Theory	27.4	46.2	50.2	46.7	75.9	80.5	79.7
Experiment	...	...	...	...	75 ± 4	...	...

[a] In kcal/mol.

TABLE VI. Barrier heights.[a]

Level of theory	$C_2H_5SiH_3 \rightarrow C_2H_5 + SiH_2$	$C_2H_5SiH_3 \rightarrow C_2H_6 + SiH_2$		$C_2H_5SiH_3 \rightarrow C_2H_4SiH_4$	$C_2H_5SiH_3 \rightarrow SiH_2{=}CHCH_3 + H_2$
		Structure C	Structure D		
HF/3-21G	79.8	94.1	84.0	109.9	132.3
HF/6-31G*	84.5	97.8	89.4	102.6	124.9
MP2/6-31G*	71.0	83.8	74.6	92.2	112.4
MP3/6-31G*	69.4	82.7	74.8	94.1	114.7
MP4/6-31G*	69.3	82.0	74.0	93.3	114.3
ΔZPE/3-21G	2.7	2.0	1.8	3.3	6.4
MP4/6-31G* + ΔZPE/3-21G	66.6	80.0	72.2	90.0	107.9

[a] Zero point energies and relative energies in kcal/mol.

the lowest thermodynamic four-center elimination pathway by -22.8 kcal/mol, owing to the more stable products that we formed (SiH_4 and C_2H_4) in the latter channel. The two most thermodynamically unfavorable channels are the homolytic cleavage of the C–C and Si–H bond, with the C–C process being 0.8 kcal/mol more stable than the Si–H bond breaking process. These two channels are more than 52 kcal/mol less favorable than the four-center elimination of SiH_4 to form ethylene reaction. However, this picture changes considerably when the kinetics of these reactions are considered.

2. Barrier heights

The calculated barriers for the various transition state structures are given in Table VI and are calculated from the total energies in Table III. Predicted barriers are compared with experiment in Table VII. The effects of basis sets on the barriers is similar to the heats of reactions, e.g., changes of ± 10 kcal/mol, upon going from the smaller (3-21G) to larger basis set (6-31G*). However, the effect of electron correlation is somewhat different, in that each barrier is reduced by 10–15 kcal/mol.

For the 1,1 hydrogen elimination to form $C_2H_5SiH + H_2$ at the Hartree–Fock level the experimental barrier height[6,7] is overestimated but inclusion of electron correlation and zero-point energy corrections brings our best estimate of the barrier height to within 1.8 kcal/mol of the barrier height measured experimentally from shock tube studies as shown in Table VII. The more extensive calculations on $SiH_2 + H_2$ [46,47] reveal that silylene insertion reactions calculated at the MP4SDQ/6-31G* level are generally in reasonable agreement with experiment, but seem to overestimate the experimental value[47] by ~ 2 kcal/mol. This is consistent with our findings for $C_2H_5SiH + H_2$.

Barrier heights calculated at all levels of theory consistently show that the relative activation energy for the 1,2-SiH_4 elimination [reaction (1)] lies about 30 ± 12 kcal/mol above that for the 1,1-hydrogen elimination reaction (3). But the three-center elimination of SiH_2 to form C_2H_6 [reaction (5)] is more favorable than the four-center elimination of SiH_4 [reaction (1)] by 17.8 kcal/mol. The least favorable pathway is the concerted elimination of molecular hydrogen to yield $SiH_2{=}CHCH_3$. The activation energy for the process is large (107.1 kcal/mol at the highest computational level). In the analogous disilane and ethane reactions, the activation energies for 1,2 elimination of H is also quite high: $CH_2{=}CH_2 + H_2$ (122.2 kcal/mol)[27] and

TABLE VII. Comparison of experimental and theoretical barrier heights.[a]

System	Method	Barrier Heights[a]	Reference
$C_2H_5SiH + H_2$	theory	66.6	this work
	experiment	65.0	6
		64.8	7
$C_2H_6 + SiH_2$	theory	72.2	this work
	experiment	70 ± 2[b]	7

[a] kcal/mol.
[b] Experimental estimate.

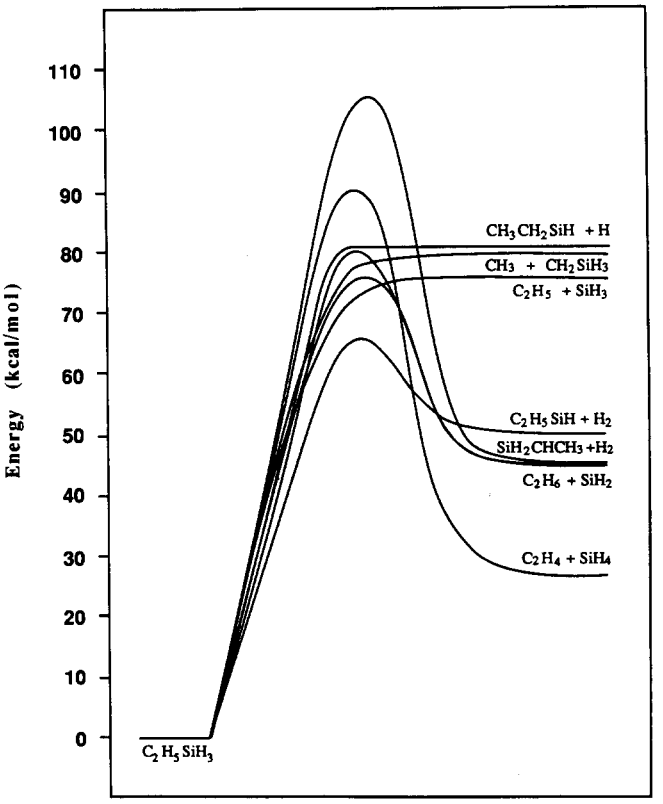

FIG. 3. Summary of potential energy curves for primary dissociation pathways for ethylsilane.

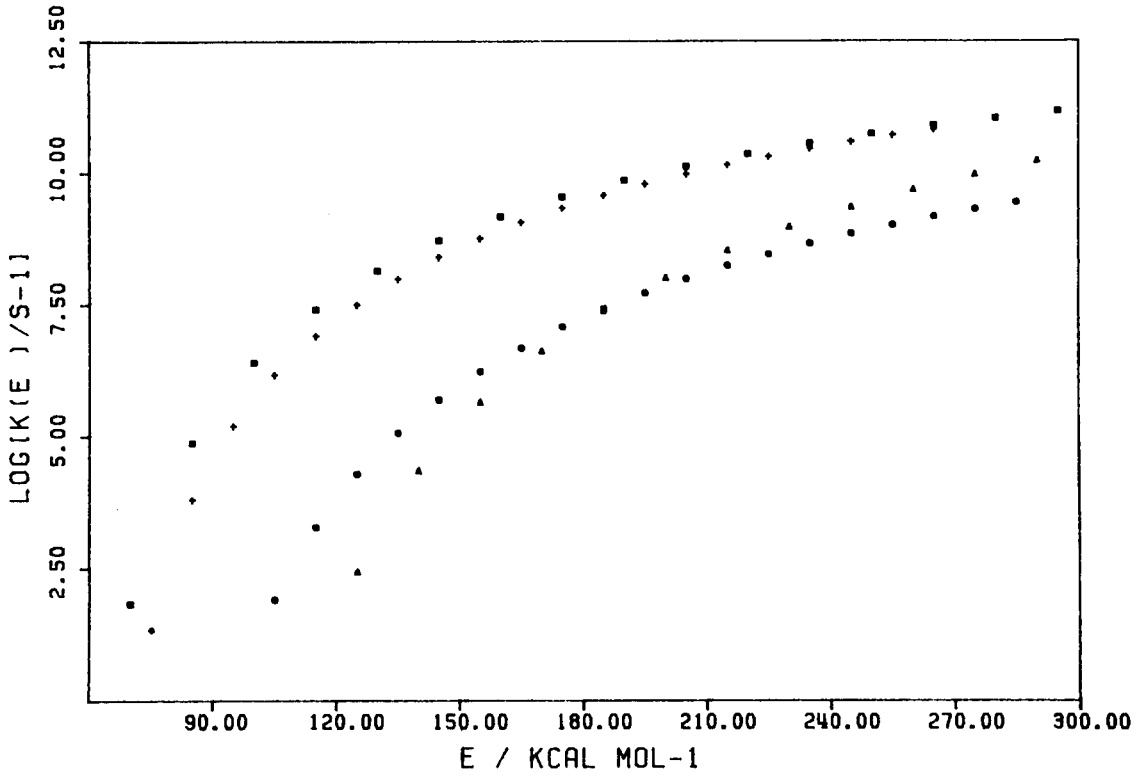

FIG. 4. Unimolecular dissociation rates for ethylsilane molecular dissociation pathways as a function energy. (■) $C_2H_5SiH + H_2$, (+) $C_2H_6 + SiH_2$, (●) $C_2H_4 + SiH_4$, (△) $SiH_2{=}CHCH_3 + H_2$.

$SiH_2{=}SiH_2 + H_2$ (86.1 kcal/mol).[28] From our estimate, $SiH_2{=}CHCH_3 + H_2$ appears to lie intermediate between these systems. A summary of the potential energy surface for ethylsilane is shown in Fig. 3.

D. RRKM calculations

In order to interpret the decomposition kinetics and assess the relative importance of channels (1)–(9), we need to know their energy dependent unimolecular dissociation rates. Such rates are obtained from RRKM theory,[48,49] in which the microcanonical unimolecular rate constant, $k_{RRKM}(E)$, of an isolated molecule possessing the total energy E is given by

$$k_{RRKM}(E) = G(E - E_0)/hN(E), \qquad (10)$$

where $G(E - E_0)$ is the sum of states for the transition state configuration, $N(E)$ the density of states for the reactant, and h is Planck's constant. The RRKM calculations are carried out using the Bunker and Hase RRKM program.[50] Harmonic state counting is employed to calculate $G(E)$ and $N(E)$ since the frequencies calculated by *ab initio* methods are determined in the harmonic approximation. The input parameters used were the frequencies for the reactant and transition states given in Table IV, the reduced internal moments of inertia for the reactant and transition states are calculated from the optimized geometries at the HF/6-31G* level of theory, and the critical energy for each pathway given in Table VI. The results of the RRKM calculations are shown in Fig. 4. Several comments can be made concerning the rate constant curves.

Over the range of 70–300 kcal/mol, the rate for the 1,1-H_2 elimination pathway [reaction (3)] appears to exceed that for all the channels considered at any assumed level of energy. This is due in part to the lower dissociation threshold for this channel compared to all other channels. At higher energies (> 100 kcal/mol), the rate constant for SiH_2 elimination competes favorably with the 1,1-H_2 elimination channel, while at even higher energies (> 250 kcal/mol), the 1,2-H_2 elimination reaction to yield $SiH_2{=}CHCH_3$ also becomes the most competitive. At lower energies it has a very minor role in the primary dissociation chemistry of ethylsilane. Rates for the four-center elimination, yielding SiH_4 and C_2H_4, are estimated to be three orders of magnitude slower than that for the 1,1-H_2 elimination reaction over the range of 95–150 kcal/mol. Taking the rate into account, the dominant pathway for decomposition is expected to be 1,1-H_2 elimination of ethylsilane.

IV. DISCUSSION: COMPARISON WITH EXPERIMENT

Previous work on the thermal and photochemical dissociation of ethylsilane has provided an unclear picture of the primary dissociation pathways for ethylsilane. Simons and co-workers[2,4] studied the decomposition of ethylsilane by chemical activation. With activated ethylsilane the main route was assumed from product balances to be the molecular 1,2 elimination to C_2H_4 and SiH_4; this assumption was not experimentally confirmed in the chemical activation studies. Although some Si–C bond rupture was also observed, more important minor pathways were suggested to

be 1,1 elimination to H_2 and C_2H_5SiH, and 1,2 hydrogen shift to SiH_2 and C_2H_6. Of these two pathways the former was considered the faster channel. Other work on halogenated ethylsilanes such as 2,2-difluoroethyltrifluorosilane between 424 to 494 K reveal that this reaction undergoes 1,2 elimination to $CHF{=}CH_2$ and SiF_4 as homogeneous first-order reaction[51] and is the dominant channel. These studies provided some supporting evidence for the assumed 1,2 elimination channel in ethylsilane. However, thermal shock tube decomposition studies of ethylsilane suggested that the dominate primary dissociation channel was 1,1-H_2 elimination.[6,7] The measured activation energy for the process compares well with our theoretical estimate as shown in Table VII. According to the yields reported for $CH_3CH{=}SiH_2$ in the shock tube experiments, the 1,2-H_2 elimination to form $CH_3CH{=}SiH_2$ should be the next competitive channel. However, according to the present calculation, the branching ratio for reactions (6) and (3) given by the ratio of the unimolecular rates should not exceed 0.0004, but the branching ratio reported from the shock tube studies is 0.45. This suggests that there is another channel for $SiH_2{=}CHCH_3$ production probably as a consequence of a 1,2-hydrogen shift from ethylsilylene:

$$CH_3CH_2SiH \rightarrow SiH_2{=}CHCH_3. \quad (11)$$

A similar process for the 1,2-hydrogen shift in methysilylene to silaethylene has been studied extensively[20,52,53]:

$$CH_3SiH \rightarrow SiH_2{=}CH_2. \quad (12)$$

Our calculations suggest that reaction (5), $C_2H_5SiH_3 \rightarrow C_2H_6 + SiH_2$, will comprise 1%–2% of the overall primary decomposition process of ethylsilane in the lower energy region. These yields are in accord with those observed in shock-tube studies[7] for this reaction and infrared multiphoton dissociation studies.[1] Unfortunately, (IRMPD) studies on ethylsilane[1,5] have been unable to unambiguously distinguish the primary photodissociation pathways. This is due to the fact that final product ratios (SiH_4 and C_2H_4) for the mechanisms involving reaction (1) and reaction (3) as primary steps give similar yields and pressure behavior. Furthermore, monitoring the SiH_2 by laser-induced fluorescence[5] shows that it is produced by secondary IRMPD during the CO_2 laser pulse, which could provide some indirect evidence for the ongoing primary dissociation channel, but even information from these studies is insufficient to resolve the issue of the lowest infrared photodissociation channel since secondary dissociation of the resulting SiH_4 and C_2H_5SiH both yield SiH_2 as a secondary photoproduct as shown below:

$$C_2H_5SiH_3 \xrightarrow{mh\nu} SiH_4^* + C_2H_4 \quad (13)$$

$$SiH_4^* \xrightarrow{m'h\nu} SiH_2 + H_2 \quad (14)$$

$$C_2H_5SiH_3 \rightarrow SiH_2 + C_2H_4 + H_2, \quad (15)$$

$$C_2H_5SiH_3 \xrightarrow{nh\nu} C_2H_5SiH^* + H_2 \quad (16)$$

$$C_2H_5SiH^* \xrightarrow{n'h\nu} C_2H_4 + SiH_2 \quad (17)$$

$$C_2H_5SiH_3 \rightarrow SiH_2 + C_2H_4 + H_2. \quad (18)$$

Consequently, these two pathways are kinetically indistinguishable for reactions occuring during the laser pulse.

The general observation in reactions induced by infrared multiphoton dissociation is that reactions proceed via the lowest thermal pathway.[54] If this is the case, then according to our calculations the primary and secondary dissociation occurring during the CO_2 laser pulse is best explained by reactions (16)–(18). Although this work suggests that the dominant primary dissociation channel for ethylsilane is decomposition to ethylsilylene and hydrogen, the principle experimental distinction between the two mechanisms is that the four-center process involves direct production of a stable primary product, SiH_4;

$$CH_3CH_2SiH \rightarrow C_2H_4 + SiH_2, \quad (19)$$

$$SiH_2 + C_2H_5SiH_3 \rightleftarrows C_2H_5SiH_2SiH_3, \quad (20)$$

$$C_2H_5SiH_2SiH_3 \rightarrow C_2H_5SiH + SiH_4 \quad (21)$$

$$\rightarrow C_2H_5SiH_2SiH + H_2, \quad (22)$$

$$C_2H_5SiH_2SiH \rightleftarrows C_2H_5SiH{=}SiH_2, \quad (23)$$

while this species is formed by secondary reactions (19)–(21) and (4) in the three-center elimination mechanism. Consequently, direct detection of SiH_4 in a crossed laser-molecular beam experiment,[55] or monitoring its formation kinetics by spectroscopic probes such as Raman scattering or diode laser absorption, would be necessary to distinguish between the two mechanisms experimentally.

ACKNOWLEDGMENTS

We are grateful to Wayne State University Computer Center and Chemistry Department for ample provision of computing resources, and W.S.U. for a Research Award (J.S.F.).

[1] J. S. Francisco, S. A. Joyce, J. I. Steinfeld, and F. Walsh, J. Phys. Chem. **88**, 3098 (1984).
[2] C. J. Mazal and J. W. Simons, J. Am. Chem. Soc. **90**, 2482 (1968).
[3] W. J. Hase, C. J. Mazal, and J. W. Simons, J. Am. Chem. Soc. **95**, 3454 (1973).
[4] T. H. Richardson and J. W. Simons, Int. J. Chem. Kinet. **10**, 1055 (1968).
[5] D. M. Rayner, R. P. Steer, P. A. Hackett, C. L. Wilson, and P. John, Chem. Phys. Lett. **123**, 449 (1986).
[6] M. A. Ring, H. E. O'Neal, S. F. Rickborn, and B. A. Sawrey, Organometallics **2**, 1891 (1983).
[7] S. F. Rickborn, M. A. Ring, and H. E. O'Neal, Int. J. Chem. Kinet. **16**, 1372 (1984).
[8] J. W. Thoman, Jr. and J. I Steinfeld, Chem. Phys. Lett. **124**, 35 (1986).
[9] J. S. Binkley, R. A. Whiteside, R. Krishnan, R. Seeger, D. J. DeFrees, H. B. Schlegel, S. Topiol, R. L. Kahn, and J. A. Pople, QCPE **13**, 406 (1980).
[10] J. S. Binkley, J. A. Pople, and W. J. Hehre, J. Am. Chem. Soc. **102**, 939 (1980).
[11] M. S. Gordon, J. S. Binkley, W. J. Pietro, and W. J. Hehre, J. Am. Chem. Soc. **104**, 2797 (1982).
[12] H. B. Schlegel, J. Comput. Chem. **3**, 214 (1982).
[13] R. Krishnan and J. A. Pople, Int. J. Quantum Chem. Symp. **14**, 91 (1980).
[14] J. A. Pople, R. Krishnan, H. B. Schlegel, and J. S. Binkley, Int. J. Quantum Chem. Symp. **13**, 225 (1979).
[15] D. H. Petersen, Ph.D. thesis, The University of Notre Dame, South Bend, Indiana, 1960.
[16] S. Nagase and T. Kudo, J. Chem. Soc. Chem. Commun. **1984**, 1392.
[17] C. Sosa and H. B. Schlegel, J. Am. Chem. Soc. **106**, 5847 (1984).
[18] I. Dubois, Can. J. Phys. **46**, 2485 (1968).
[19] M. S. Gordon, J. Am. Chem. Soc. **104**, 4352 (1982).

[20]Y. Yoshioka, J. D. Goddard, and H. F. Schaefer, J. Am. Chem. Soc. **103**, 2542 (1981).
[21]P. G. Mahaffy, R. Gutowsky, and L. K. Montgomery, J. Am. Chem. Soc. **102**, 2854 (1980).
[22]N. Wiberg, G. Wagner, and G. Mullen, Agnew Chem. Int. Ed. Eng. **24**, 229 (1985).
[23]M. E. Colvin, J. Kobayaski, J. Bicerano, and H. F. Schaefer, J. Chem. Phys. **85**, 4563 (1986).
[24]T. J. Barton, A. Resis, I. M. T. Davidson, S. I. Maghsoodi, K. J. Hughes, and M. S. Gordon, J. Am. Chem. Soc. **108**, 4022 (1987).
[25]M. S. Gordon and T. N. Truong, Chem. Phys. Lett. **142**, 110 (1987).
[26]C. Gonzales, H. B. Schlegel, and J. S. Francisco (to be published).
[27]M. S. Gordon, T. N. Truong, and J. A. Pople, Chem. Phys. Lett. **130**, 245 (1986).
[28]M. S. Gordon, T. N. Truong, and E. K. Bonderson, J. Am. Chem. Soc. **108**, 1421 (1986).
[29]M. S. Gordon (to be published).
[30]K. M. MacKay and R. Watt, Spectrochim. Acta Part A **23**, 2761 (1967).
[31]J. R. Durig, P. Groner, and A. D. Lopata, Chem. Phys. **21**, 401 (1977).
[32]J. A. Pople, H. B. Schlegel, R. Krishnan, D. J. DeFrees, J. S. Binkley, M. J. Frisch, R. A. Whiteside, R. F. Hout, and W. J. Hehre, Int. J. Quantum. Chem. Symp. **15**, 269 (1981).
[33]M. S. Gordon, D. R. Gano, J. S. Binkley, and M. J. Frisch, J. Am. Chem. Soc. **108**, 2191 (1986).
[34]S. R. Gunn and L. H. Green, J. Phys. Chem. **65**, 779 (1961).
[35]A. M. Doncaster and R. Walsh, Int. J. Chem. Kinet. **13**, 503 (1981).
[36]J. Berkowitz, J. P. Greene, H. Cho, and B. Ruscic, J. Chem. Phys. **86**, 1235 (1987).
[37]J. S. Francisco, R. Barnes, J. W. Thoman, Jr., J. Chem. Phys. (to be published).
[38]F. D. Rossini and J. W. Knowlton, J. Res. Natl. Bur. Stand. **19**, 249 (1937).
[39]G. B. Kistiakowsky, H. Romeyn, J. R. Ruhoff, H. A. Smith, and W. E. Vaughan, J. Am. Chem. Soc. **57**, 65 (1935).
[40]D. M. Golden and S. W. Benson, Chem. Rev. **69**, 125 (1969).
[41]A. C. Castelhano, P. R. Marriott, and D. Griller, J. Am. Chem. Soc. **103**, 4263 (1981).
[42]W. Doering, Proc. Natl. Acad. Sci. U.S.A. **78**, 5279 (1981).
[43]D. A. Parks and C. P. Quinn, J. Chem. Soc. Faraday Trans. 1 **72**, 1952 (1976).
[44]A. C. Baldwin, I. M. T. Davidson, and M. D. Reed, J. Chem. Soc. Faraday Trans. 1 **74**, 2171 (1978).
[45]R. Walsh, Acc. Chem. Res. **14**, 246 (1981).
[46]H. B. Schlegel and C. Sosa, J. Phys. Chem. **89**, 537 (1985).
[47]M. S. Gordon, J. Chem. Soc. Chem. Commun. **1981**, 890.
[48]R. A. Marcus, J. Chem Phys. **20**, 359 (1952).
[49]P. J. Robinson and K. A. Holbrook, *Unimolecular Reactions* (Wiley–Interscience, New York, 1972).
[50]W. L. Hase and D. L. Bunker, Program 234, Quantum Chemistry, Program Exchange, Indiana University, Bloomington (1973).
[51]R. N. Haszeldine, P. J. Robinson, and R. F. Simmons, J. Chem. Soc. **1964**, 1890.
[52]J. D. Goddard, Y. Yoshioka, and H. F. Schaefer, J. Am. Chem. Soc. **102**, 7644 (1980).
[53]M. S. Gordon, Chem. Phys. Lett. **54**, 9 (1978).
[54]J. S. Francisco and J. I. Steinfeld, in *Advances in Multiphoton Processes and Spectroscopy*, edited by S. H. Lin (Taylor and Francis, London, 1986), pp. 79–175.
[55]J. S. Francisco, G. Reck, and J. Villanueva (to be published).